Macromolecules

Article

pubs.acs.org/Macromolecules

Challenging Tube and Slip-Link Models: Predicting the Linear Rheology of Blends of Well-Characterized Star and Linear 1,4-Polybutadienes

Priyanka S. Desai,[†] Beom-Goo Kang,[§] Maria Katzarova,[∥] Ryan Hall,[†] Qifan Huang,[‡] Sanghoon Lee,[#] Maksim Shivokhin,[∥] Taihyun Chang,[#] David C. Venerus,[∥] Jimmy Mays,[§] Jay D. Schieber,[∥,⊥] and Ronald G. Larson*[,†,‡]

[†]Department of Macromolecular Science & Engineering and [‡]Department of Chemical Engineering, University of Michigan, Ann Arbor, Michigan 48109, United States

[§]Department of Chemistry, University of Tennessee, Knoxville, Tennessee 37966, United States

[∥]Department of Chemical and Biological Engineering, and Center for Molecular Study of Condensed Soft Matter, and [⊥]Department of Physics, Illinois Institute of Technology, Chicago, Illinois 60616, United States

[#]Department of Chemistry and Division of Advanced Materials Science, Pohang University of Science and Technology (POSTECH), Pohang 37673, Korea

Supporting Information

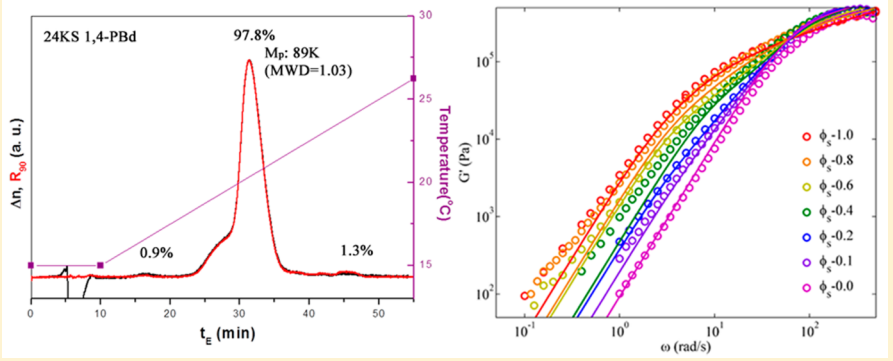

ABSTRACT: We compare predictions of two of the most advanced versions of the tube model, namely the "Hierarchical model" by Wang et al. [*J. Rheol.* **2010**, *54*, 223] and the BoB (branch-on-branch) model by Das et al. [*J. Rheol.* **2006**, *50*, 207], against linear viscoelastic G' and G'' data of binary blends of nearly monodisperse 1,4-polybutadiene 4-arm star polymer of arm molar mass 24 000 g/mol with a monodisperse linear 1,4-polybutadiene of molar mass 58 000 g/mol. The star was carefully synthesized and characterized by temperature gradient interaction chromatography and by linear rheology over a wide frequency region through time−temperature superposition. We found large failures of both the Hierarchical and BoB models to predict the terminal relaxation behavior of the star/linear blends, despite their success in predicting the rheology of the pure star and pure linear polymers. This failure occurred regardless of the choices made concerning constraint release, such as assuming arm retraction in "fat" or "skinny" tubes. Allowing for "disentanglement relaxation" to cut off the constraint release Rouse process at long times does lead to improved predictions for our blends, but leads to much worse predictions for other star/linear blends described in the literature, especially those of Shivokhin et al. [*Macromolecules* **2014**, *47*, 2451]. In addition, our blends and those of Shivokhin et al. were also tested against a coarse-grained slip-link model, the "clustered fixed slip-link model (CFSM)" of Schieber and co-workers [*J. Rheol.* **2014**, *58*, 723], in which several Kuhn steps are clustered together for computational efficiency. The CFSM with only two molecular-weight- and chain-architecture-independent parameters was able to give very good agreement with all experimental data for both of these sets of blends. In light of its success, the CFSM slip-link model may be used to address the constraint release issue more rigorously and potentially help develop improved tube models.

I. INTRODUCTION

The introduction of a mean-field entanglement "tube" to describe constraints on polymer motion by de Gennes[1] and Doi and Edwards[2] has greatly advanced our understanding of the dynamics and rheology of polymers with various complex

Received: December 4, 2015
Revised: May 31, 2016
Published: June 21, 2016

DOI: 10.1021/acs.macromol.5b02641
Macromolecules 2016, 49, 4964−4977

architectures and of their blends. In the tube model, relaxation occurs by chain motion within the tube and by release of the entanglement constraints that define the tube. Motion within the tube has been described by a combination of reptation or sliding of the whole chain along the tube and by contour length fluctuations, or "breathing modes", which allow the ends of the chain to escape the ends of the tube and relax stress faster than by reptation alone. Constraint release can be modeled for polydisperse linear polymers by allowing the tube itself to undergo local diffusion due to repeated release of constraints along its contour. The motion of the tube produced by the accumulation of local constraint-release events is mathematically identical to Rouse relaxation, except that "viscosity" of the medium through which the Rouse "chain" (actually tube) drifts is set by the rate at which constraints are released by the surrounding chains.[3] Hence, this mechanism is called "constraint-release (CR) Rouse relaxation". CR-Rouse relaxation, however, is not adequate to describe constraint release effects for monodisperse star polymers. For these, it has been necessary to introduce the concept of "tube dilation" (also known as dynamic dilution[4]), which envisages that constraint release gradually enlarges the diameter of the tube constraining the polymer, shortening its length, and thus accelerating the relaxation of the chain within it.

A "universal" tube model capable of describing all well-entangled polymers, including mixtures of branched and linear polymers, is a "Holy Grail" of rheological modeling, since such a theory would allow commercial polymer melts to be modeled reliably. In an effort to develop such a model, it is necessary to describe constraint release for blends of branched and linear polymers. As a first effort in this direction, Milner, McLeish, and co-workers[5] used a combination of tube dilation and CR-Rouse relaxation to predict constraint release dynamics of a blend of a monodisperse star polymer with a monodisperse linear polymer, with CR-Rouse processes controlling the rate at which the dynamic dilution of the star arms proceeds. Their work was a crucial step toward the development of general tube theories for relaxation of mixtures of linear and long-chain-branched polymers of arbitrary branching structure. Two such general theories, the "Hierarchical" model of Larson and co-workers, and the "BoB" (branch-on-branch) model of Das, McLeish, Read, and co-workers, are now publically available and have enjoyed some success in predicting the rheology of complex mixtures of branched and linear polymers.

Despite these advances in understanding, there are significant difficulties and ambiguities in accounting for constraint release within tube models. Sometimes reptation or fluctuations of the chain are taken to occur in an undilated "skinny" tube[6] and sometimes in the dilated "fat" tube,[7] and it is unclear in general which tube diameter to use. In the original work of Milner et al.[5] that first addressed star−linear blends, constraint release caused by relaxation of the linear chains dynamically widens the tube containing the star arm, but during this widening the fluctuations of that arm are mysteriously shut off, until the widening comes to an end. This is the so-called "arm frozen" assumption, also adopted by Park et al.[8] Apart from its producing relatively good agreement between model and experiment for the particular set of star/linear blends studied by Milner and McLeish, there seems little justification for this assumption. In addition, during constraint release caused by relaxation of the linear chains, there are two commonly used choices for the value α of the tube diameter "dilution exponent" relating tube diameter to the fraction of unrelaxed melt. The value $\alpha = 4/3$ can be obtained by scaling arguments and contrasts with the value $\alpha = 1$ which arises from the assumption that entanglements are binary events. In general, the value $\alpha = 1$ appears to be required to obtain agreement with data for binary blends of linear polymers, while accurate prediction of the rheology of star polymers seems to require setting $\alpha = 4/3$, at least in some tube models.[9] When the artificial "arm frozen" assumption is removed and the arms are allowed to fluctuate in a thin tube during the CR-Rouse process, tube theories are able to predict the rheology of both linear and star polymers when $\alpha = 4/3$, but the star/linear blend is rather poorly described, as discussed by Wang et al.[9]

In addition to these issues with star/linear blends, recent work by van Ruymbeke et al.[10] on linear/linear binary blends suggests that the dilution exponent α might need to be made a function of time, changing from 1 at early times to 4/3 at late times. Khaliullin and Schieber[11] recently showed that two different versions of the tube model were unable to give an accurate prediction of binary linear blends. In addition, recent work of Watanabe[12] suggests that even for "simple" cases of linear/linear blends, previous theories of constraint release effects are inadequate. Thus, the inclusion of constraint release mechanisms within the tube model is problematic, especially for star/linear blends, where constraint release is described by a combination of CR-Rouse processes and tube dilation.

We note, however, that there are only two "complete" data sets in the current literature for blends of monodisperse star and linear 1,4-polybutadiene polymers as well as one set of star-linear blends of monodisperse polyisoprenes.[60] The 1,4-polybutadiene star/linear blend studied theoretically by Milner, McLeish, and co-workers is a blend that we here call "PBd42.3KS-105KL", containing a monodisperse star polymer having arm molar mass 42 333 g/mol and a monodisperse linear polymer having molar mass 105 000 g/mol. This data set was taken from the work of Struglinski et al.[13] There is also a very recent 1,4-polybutadiene data set, here called "PBd27.4KS-6.9KL" of Shivokhin et al.[14] with star arm reportedly having molar mass 27 400 g/mol, and the linear molecule having molar mass 6900 g/mol, which is only high enough to be modestly self-entangled.[14] Other, less complete, data sets for star/linear blends include the 1,4-polybutadiene blends of Lee and Archer[15] and of Roovers.[16] However, the former data set does not include rheological data for the pure star, while the latter only contains data for a blend of 2.5% star in a linear matrix. Hence, to assess tube models more thoroughly, there is a great need for additional data sets on well-entangled blends of nearly monodisperse star and linear polymers, which motivates our acquisition of a new, complete, data set here.

In part because of the unsatisfactory treatment of constraint release within the tube model, in recent years an alternative to the tube model, the so-called "slip-link" class of models, has attracted increasing attention.[17−23] Slip-link models track the stochastic motion of individual chains and average over many such chains to obtain the rheological response. Most importantly, in slip-link models the constraints on chain motion imposed by entanglements are accounted for individually, rather than collectively, as in the tube model.[20] Thus, the "tube", which confines the chain *globally* along its length, is replaced by "slip-links" that *locally* constrain chain sliding to pass through the position of each slip-link. Both reptation and local Rouse motions along chains are captured naturally in slip-link models as a result of their more-detailed level of description; they are not imposed a priori as in tube

DOI: 10.1021/acs.macromol.5b02641
Macromolecules 2016, 49, 4964−4977

Table 1. Synthesis of 4-Arm Star PBd at Room Temperature in Benzene[a]

				4-arm star PBd (PBd)		
				M_n (kg/mol)		
sample	*s*-BuLi (mmol)	Bd (mmol)	BMDCSE (mmol)	calcd[b]	obsd[c]	M_w/M_n[c]
24KS	0.55	222	0.11	88 (22)	97 (24)	1.05 (1.04)

[a]Yields of polymers were quantitative. [b]M_n(calcd) of PBd = (molecular weight of monomer) × [monomer]/[initiator]. M_n(calcd) of 24KS = M_n(calcd) of PBd × 4. [c]M_n(obsd) and M_w/M_n were obtained by SEC-TALLS using THF as an eluent.

models. Constraint release arises through the disappearance of slip-links when chain ends pass through a slip-link and is balanced by the appearance of new slip-links by detailed balance. A major advantage of slip-link models is that in doing away with the tube, no explicit accounting need be made of "tube dilation" or of CR-Rouse tube motion. Instead, these processes are allowed to arise naturally from the constrained motion of the chains and the appearance and disappearance of slip-links.

While slip-link models remove many of the questionable assumptions involved in the tube model discussed above, they do replace these with the assumption that entanglements can be described as discrete topological interactions, each of which involves only two chains.[21,22] Some slip-link models (excluding the CFSM discussed below) also enact additional algorithmic rules beyond those needed to represent mathematical expressions to determine when and how neighboring chains become "entangled" and new slip-links are added.[17,23] In addition, slip-link models are computationally much more demanding than tube models. In fact, for star molecules, which relax very slowly, most slip-link models can simulate molecules with only 5 or 10 entanglements per branch,[24] although a recent more coarse-grained slip-link model by Schieber and co-workers, the clustered fixed slip-link model[25] (CFSM), can simulate stars with 19 or more entanglements, as is the case for the star studied in this work. Recent implementation of a GPU algorithm[26] for simulations using the slip-link model will increase the model's capabilities further still.

To progress further, it is important to obtain additional high quality data for well-entangled blends of monodisperse star and monodisperse linear polymers and to compare these data against the most advanced tube and slip-link models. To make the blends more accessible to analysis by slip-link models, it is important that the star arms be reasonably short, while remaining well entangled.

In this paper, therefore, we describe the synthesis and characterization of a monodisperse 1,4-polybutadiene star of arm molar mass around 24 000 g/mol. Since the rheological data obtained from this material are intended to be used to test models, and since star polymers are extremely sensitive to impurities, especially of linear contaminants, this star is characterized by both size exclusion chromatography (SEC) and temperature gradient interaction chromatography (TGIC). It contains four arms, so that if some small fraction of the molecules lack an arm, or have an excess arm, this will have little effect on the rheology. (It is well established that the rheology of star polymers is mainly sensitive to arm molecular weight, not to the number of arms, so long as the number of arms is roughly between 3 and 33.[27]) The relatively modest molecular weight of this star polymer material makes it amenable to analysis using slip-link models, especially when blended with linear polymer. To prepare well-controlled blends, a linear 1,4-polybutadiene polymer of molar mass 58 000 g/mol is acquired commercially and also characterized rheologically to ensure its quality. The rheological measurements on the pure star and pure linear materials are carried out on two rheometers, one of which is equipped with a low-temperature fixture so that high-frequency data can be obtained by time–temperature superposition (TTS). The experiments are performed at low temperatures for three reasons: (i) to ensure that rheological data for the two materials superpose in the high-frequency regime, (ii) to ensure that the material remains chemically stable during the rheological measurements, and (iii) to allow the established value of the "equilibration time" for 1,4-polybutadiene to be affirmed.

Mixtures of these star and linear materials, forming "PBd24KS-58KL" blends, are then also studied rheologically, and the data used to test two modern tube theories for linear viscoelastic properties, namely the "Hierarchical 3.0" model by Wang et al.[9] and BoB (branch-on-branch) model by Das et al.[6] Both models have previously been shown to be successful in quantitatively describing the rheological properties of a range of polymers, including "combs", hyperbranched polymers, and commercial polyolefins made by single-site metallocene catalysis, but were not able to describe accurately the rheology of the PBd42.3KS-105KL blends. However, the PBd42.3KS-105KL is not amenable to analysis by slip-link models at present because of the large number of entanglements in the star polymer. Our aim here is to see how well both the tube model and the slip-link model can predict the rheology of a star–linear blend. The PBd24KS-58KL blends are ideal for this purpose, given the recent development of a relatively fast slip-link model, discussed below.[25]

The article is outlined as follows. Section II describes the detailed synthesis and TGIC characterization of the pure 4-arm star 1,4-PBd of arm molar mass 24 000 g/mol and its blend preparation with a linear 1,4-PBd of molar mass 58 000 g/mol along with their experimental rheology characterization. In section III, we describe the tube model theory and the slip-link simulations. In section IV, we present and discuss experimental rheological measurements and compare and contrast the massive failure we observe of the tube theories to predict the star/linear rheological data with the successful predictions of the slip-link model. Conclusions and perspectives are presented in section V.

II. MATERIALS AND EXPERIMENTAL METHODS

II.1. Materials and Blends Preparation. Two 1,4-polybutadienes, namely a linear and a star sample, as well as their blends, were used in this study. The linear 1,4-PBd was purchased from Polymer Source, Inc. Its number-average molecular weight and molecular weight distribution were reported by Polymer Source to be 58 000 g/mol and 1.03, respectively, and its chemical composition of cis-1,4, trans-1,4, and 1,2-vinyl was given as 68%, 27%, and 5%, respectively. We refer to the linear sample as "58KL". A four-arm symmetric 1,4-PBd star was synthesized as described in detail in the following section. Its arm number-average molecular weight and molecular weight

DOI: 10.1021/acs.macromol.5b02641
Macromolecules 2016, 49, 4964–4977

distribution are 24 000 g/mol and 1.04, respectively, and we refer to it as "24KS". The molecular characteristics of the symmetric 4-arm star sample are given in Table 1. 1,4-PBd star/linear blends were prepared at star weight fractions 80%, 60%, 40%, 20%, and 10%. Weighed amounts of linear and star melts were dissolved in excess dichloromethane (sourced from Sigma-Aldrich). The solvent was initially allowed to evaporate from the sample at atmospheric pressure in a fume hood for about a week, and then the sample was transferred to a vacuum chamber held at room temperature for another 2 weeks or more to ensure complete removal of excess dichloromethane. The blends were checked for remaining solvent via smell after drying under vacuum, and the weight of the samples was monitored over 3 days to ensure complete solvent removal and to produce the final star/linear melt blends with desired compositions. After vacuum drying, the blends were stored in the freezer prior to rheological measurements.

II.2. Synthesis and Purification. 1,3-Butadiene (Bd) (Aldrich, 99%), benzene (Aldrich, 99.8%), and methanol (terminating agent, Aldrich, 99%) were purified according to experimental techniques common in high-vacuum anionic polymerization.[28−31] 1,2-Bis(methyldichlorosilyl)ethane (BMDCSE) (linking agent, Gelest, 95%) was distilled several times over CaH_2 on a vacuum line. *sec*-Butyllithium (*s*-BuLi, 1.4 M in cyclohexane, Aldrich) was used without purification and was diluted with dry *n*-hexane. The diluted reagents were stored at −30 °C in ampules equipped with break-seals before use. The polymerization and linking reaction were performed under high vacuum conditions in the sealed all-glass reactors equipped with break-seals. The reactors were prewashed with *n*-BuLi solution after sealing off from the vacuum line.

II.2.i. Synthesis of Living PBd. The polymerization of Bd (12 g, 222 mmol) was performed using *s*-BuLi (0.55 mmol) in benzene at room temperature for 24 h (Scheme 1a). Then, a small portion of living

Scheme 1. Synthetic Route for 4-Arm Star PBd (24KS)

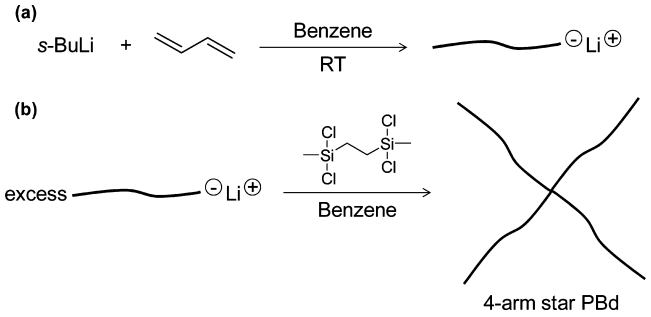

PBdLi was sampled by heat-sealing the constriction for characterization. The rest of living polymer solution was subsequently gathered in a precalibrated ampule equipped with break-seals for the linking reaction with BMDCSE. The resulting PBd was characterized by SEC, giving PBd (M_n(obsd) = 24 kg/mol, M_w/M_n = 1.04 (Table 1)).

II.2.ii. Synthesis of 4-Arm Star PBd (24KS). The linking reaction of a benzene solution of living PBd (24 kg/mol, 0.5 mmol) with the linking agent BMDCSE (0.11 mmol) was performed in benzene (500 mL) at room temperature for 3 weeks with rigorous stirring to form well-defined 4-arm star PBd. The reaction was monitored by sampling a small amount of reaction solution via constrictions for SEC characterization. After terminating the linking solution with degassed methanol, the polymer solution was stabilized with butylated hydroxytoluene (BHT) and then poured into a large excess of methanol to precipitate the polymers. The fractional precipitation was repeated using toluene/MeOH to isolate highly pure 4-arm star PBd. The fractionated star polymer was further precipitated in methanol and dried under high vacuum conditions for characterization. The resulting 4-arm star PBd was characterized by SEC, giving 24KS (M_n(obsd) = 97 kg/mol, M_w/M_n = 1.05 (Table 1)).

II.3. SEC and TGIC Characterization. *II.3.i. Size Exclusion Chromatography (SEC).* Size exclusion chromatography/two-angle laser light scattering (SEC-TALLS) connected with a refractive index (RI) detector and Viscotek differential viscometer was used to characterize the star arm, PBd, and 4-arm star PBd, 24KS. Tetrahydrofuran (THF) was used as the mobile phase at a flow rate of 1.0 mL/min at 40 °C. This system features a Waters 1525 high-pressure pump, Waters Ultrastyragel columns (HR-2, HR-4, HR-5E, and HR-6E with pore sizes 10^3, 10^4, and 10^5 Å), a Waters 2410 differential refractometer detector (at 680 nm), a Precision Detectors PD-2040 two-angle (15°, 90°) light scattering detector, and a Viscotek differential viscometer. The Precision Detectors software "Discovery 32" was utilized to calculate the M_w values from SEC-TALLS data. The refractive index increment (dn/dc) value was measured on a Wyatt Optilab DSP detector at a wavelength of 690 nm and temperature of 40 °C in THF. After dn/dc was measured for five different concentrations of each sample, the average value 0.130 mL/g was used.

II.3.ii. Temperature Gradient Interaction Chromatography (TGIC). TGIC is an HPLC technique controlling the interaction strength of the analytes with the stationary phase by changing the temperature of the column.[32,33] TGIC experiments were carried out with a typical HPLC system equipped with a C18 bonded silica column (Nucleosil C18, 250 × 4.6 i.d. mm, 500 Å, 7 μm particle size). The eluent was 1,4-dioxane (Samchun, HPLC grade) at a flow rate of 0.4 mL/min. The temperature of the column was controlled by circulating a fluid from a programmable bath/circulator (Thermo-Haake, C26P) through a homemade column jacket. All TGIC analyses were done with a linear temperature gradient from 15 to 30 °C in 60 min (0.25 °C/min). Sample solutions in 1,4−dioxane (~3 mg/mL, dn/dc = 0.104 mL/g) were prepared by dissolving the polymers in a small volume of the eluting solvent and the injection volume was 100 μL.[34] The TGIC chromatograms were recorded with a differential refractometer (RI) detector (Shodex, RI-101) and a light scattering (LS) detector (Wyatt, miniDawn).

II.4. Synthesis of 4-Arm Star PBd (24KS), SEC and TGIC Characterization Results. *II.4.i. Synthesis of 4-Arm Star PBd (24KS).* Scheme 1 shows the synthetic strategy to prepare the well-defined 4-arm star PBd. First, the polymerization of Bd was carried out to synthesize living PBd (Scheme 1a). The colorless polymerization solution of Bd was maintained for 24 h. The polymerization results shown in Figure 1 and Table 1 suggest that the well-defined PBd was

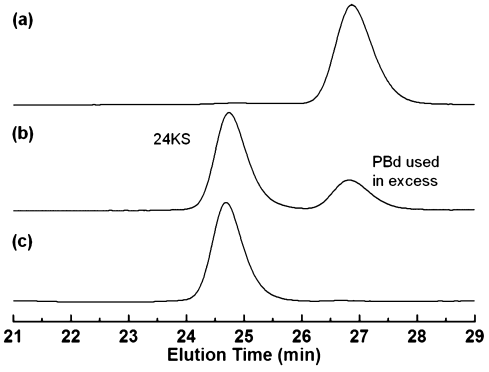

Figure 1. SEC curves of (a) PBd (i.e., the linear arms), (b) the polymer mixture obtained from the linking reaction, and (c) 24KS after fractional precipitation.

successfully synthesized, as expected. The observed M_n value agrees well with predicted one based on monomer-to-initiator ratios, and the SEC curve of PBd shows a unimodal shape with narrow M_w/M_n (Figure 1a).

Next, the synthesis of 24KS was performed by the reaction of excess living PBd with BMDCSE (Scheme 1b). In this procedure, it should be noted that careful purification of BMDCSE via repeated distillations on a vacuum line is necessary to obtain a highly pure linking agent, which is the key factor for synthesis of the desired 24KS. The reaction was monitored by SEC analysis. The reaction was considered complete when the SEC peak of PBd used in excess did not change (Figure 1b). As shown in Figure 1c, highly pure 24KS was finally obtained from

DOI: 10.1021/acs.macromol.5b02641
Macromolecules 2016, 49, 4964−4977

fractional precipitation. Although the controlled M_n and narrow M_w/M_n of 24KS demonstrate that a well-defined 4-arm star PBd was synthesized under the reaction conditions employed in this study (Table 1), SEC is not able to distinguish impurities caused by incomplete or excess linkage of arms to the linking agent. We therefore also characterize the sample by temperature gradient interaction chromatography (TGIC), which is able to detect such impurities, as discussed below.

II.4.ii. Characterization of 4-Arm Star PBd (24KS) by TGIC. TGIC is known to separate polymers according to their molecular weight (MW) while SEC separates them according to the hydrodynamic size.[32] In addition, TGIC shows much higher resolution than SEC in resolving the branched polymers prepared by anionic polymerization according to their MW.[35−37] Therefore, we employed TGIC to further characterize the 24KS sample since rheological properties are very sensitive to the chain branching and TGIC can resolve the star-shaped polymers far better than SEC.[38,39]

Figure 2 shows TGIC chromatogram of 24KS. It was recorded by an RI detector (Δn) and LS detector at 90° scattering angle (R_{90}) to

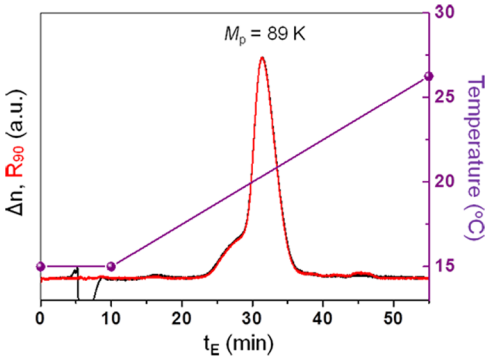

Figure 2. RP-TGIC chromatogram of 24KS (after fractional precipitation) recorded by a RI detector (black line) and a LS detector (red line). Peak MW (M_p) is determined by LS detection. Column temperature program is also shown in the plots.

measure the absolute MW. The peak MW (M_p) of 24KS was measured to be 89 kg/mol, which agrees reasonably well with the value determined by SEC-TALLS (97 kg/mol). 24KS shows a main peak eluting out at 30−35 min and a large fronting shoulder eluting out at 25−30 min (Figure 2). The shape of the peak indicates that 24KS contains a significant amount of byproduct eluting in its shoulder, but it appears quite uniform in MW judging from the well-overlapped RI and LS signals. Such an overlap of concentration and LS signals is a good indication of very narrow MW distribution.[39] A possible explanation of the peculiar behavior is that the polymers eluting in the fronting shoulder are the same in molecular weight as those in the main peak but contain a functionality which is repulsively interacting with the C18 stationary phase.[40]

The linking agent, BMDCSE, can undergo hydrolysis/oligomerization during the storage to become a linker with more than four chlorosilyl groups. The oligomerized BMDCSE could result in byproducts of stars with more than 4 arms and/or additional functionality such as hydroxy group(s). The high-MW species (stars with more than 4 arms) were well removed by the fractional precipitation, but 4-arm star PBd with additional functionality remains and might be detected in the TGIC analysis.[41] This scenario is supported by the TGIC chromatogram of 24KS shown in Figure 2. In the chromatogram, a trace of high-MW species was found after the main peak. The amount is almost negligible, but certainly higher than the noise level. The values of molar masses given by SEC-TALLS and TGIC are 97 and 89 kg/mol, respectively, both of which are within experimental error of the target molar mass of 24 000 g/mol per arm or 96 000 g/mol for the whole polymer.

II.5. Rheology Experiments. Dynamic storage $G'(\omega)$ and loss $G''(\omega)$ moduli for the star/linear PBd blend samples were measured in small-amplitude oscillatory shear flow using the strain-controlled ARES-LS rheometer with a 8 mm diameter parallel plate and at a sample gap of 1 mm. Dynamic strain sweep measurements were first conducted to select the strains in the linear regime. Dynamic frequency sweeps were conducted at a constant temperature of 25 °C at frequencies ranging from 0.01 to 100 rad/s using a strain amplitude of 10%. In order to ensure sample stability, a gaseous nitrogen atmosphere was used. For the case of pure star, 24KS, and pure linear 58KL samples, linear viscoelastic oscillatory shear tests were also carried out on the Rheometrics mechanical spectrometer RMS-800, using an 8 mm parallel plate geometry at frequencies ranging from 0.1 to 100 rad/s and temperatures from +25 to −80 °C under a liquid nitrogen blanket. Linear viscoelastic $G'(\omega)$ and $G''(\omega)$ curves from oscillatory experiments at various low temperatures were then horizontally shifted using the time−temperature superposition (TTS) software on the rheometer using a two-dimensional residual minimization technique to form a master curve at a reference temperature of +25 °C. From this, the WLF (Williams−Landel−Ferry) shift factors $a_T(T)$ were obtained at multiple measurement temperatures for both 24KS and 58KL samples.

III. THEORY, MODELING, AND SIMULATIONS

III.1. Tube Models. We test constraint release dynamics using two coarse-grained mean-field tube models that were developed for predicting the linear rheology of general mixtures of branched polymers. The first is the Hierarchical 3.0 model by Wang et al.,[9] and the second is the BoB (branch-on-branch) model by Das et al.[6] Even though both models are based on similar hierarchical relaxation mechanisms and treatment of constraint release dynamics, they differ in their computational algorithms and implementation, a detailed comparison of which is presented in Wang et al.[9] In the Appendix (Supporting Information), we also test a model that implements the original equations of Milner et al.[5] designed for star/linear blend rheology.

The predictions are carried out using two sets of parameter values summarized in Table 2. The so-called "Park" values,

Table 2. Input Parameters Used in Hierarchical and BoB Model Calculations of 1,4-PBd at T = 25 °C

parameters	Hierarchical 3.0 Park parameters	BoB Das parameters
α	4/3	1
G_N^0 (MPa)	1.15	0.97
M_e (Da)	1650	1836
τ_e (s)	3.7×10^{-7}	2.75×10^{-7}

from the work of Park et al.[8] and Wang et al.,[9] are used as input parameters for the Hierarchical model and the "Das" values, from Das et al.,[6] are used with the BoB model. In both of the models, the two most important material dependent parameters, the plateau modulus G_N^0 and the entanglement molecular weight M_e, are related to each other by the definition $M_e = (4/5)\rho RT/G_N^0$. Another fundamental tube model parameter, τ_e, the equilibration time or Rouse relaxation time of a chain containing one entanglement, was obtained by adjusting its value to best fit the low frequency data in both the models. By fitting the Rouse model to the high-frequency transition linear viscoelastic data for a series of 1,4-PBd samples, Park et al.[42] recently determined the value of τ_e and its uncertainty as $(3.7 \pm 0.93) \times 10^{-7}$ s at T = 25 °C for 1,4-PBd, and both the Park and Das values for τ_e lie within these limits. Perhaps the best-known difference between both these parameter sets is in the value of the so-called "dilution exponent" α, which controls the rate at which the tube expands its diameter as polymer chains relax.[43]

DOI: 10.1021/acs.macromol.5b02641
Macromolecules 2016, 49, 4964−4977

Details describing the tube dilation process can be found in Milner and McLeish.[44] Two different theoretical concepts—one that focuses on entanglements as pairwise interactions between chains and the other one treating entanglements as a collective phenomenon[45]—give the two values $\alpha = 1$ and $\alpha = 4/3$ that are used in the Das and Park parameter sets, respectively. While these two values are similar, they are exponents on a quantity that is itself inside an exponential function, and therefore a small difference between them has a big impact on predictions. We remark here that there is another set of input parameters explored by Park and Larson[57] in which $\alpha = 1$ is used that is similar to the parameter set used in the original paper of Milner et al.[5] We test this parameter set in the Appendix and find that while it improves predictions somewhat for the data set studied in Milner et al.,[5] it does not improve the predictions of the tube model for the new blends studied here.

The Hierarchical model gives the user the freedom to choose between three different arm retraction algorithms, wherein the arm contained within the tube may relax by retraction while the confining tube itself undergoes CR-Rouse motion. These options are the following. (1) No arm retraction: arm retraction is not allowed or is "frozen" during CR-Rouse motion. (2) Arm retraction in the "thin" tube: arm retraction occurs in the thin tube whose diameter is defined by the unrelaxed volume fraction, ϕ, just before the onset of CR-Rouse motion. (3) Arm retraction in the "fat" tube: the arm retracts in a "fat" tube whose diameter is set by $\phi_{ST}(t)$, which is the fraction of original entanglements that define the tube that the arm is able to explore by constraint release during a time t. The fat fraction ϕ_{ST} is either allowed to decrease with the inverse of the constraint-release Rouse relaxation rate, or if this would bring ϕ_{ST} below ϕ, then ϕ_{ST} is simply set equal to ϕ. Details regarding these options are given in Wang et al.[9] Here we test the "thin tube" and the "fat tube" as well as the "arm frozen option" in the Hierarchical model and results are discussed below. The BoB model, on the other hand, does not give these options and arm retraction proceeds in the "thin" tube, which is the same as option 2 in the Hierarchical model.

III.2. Slip-Link Predictions. *III.2.i. Discrete Slip-Link Model.* The discrete slip-link model (DSM) is a single-chain mean-field model for entanglement-dominated polymer dynamics proposed by Schieber and co-workers.[22,46,47] The model has been shown to be consistent with thermodynamics.[48] With just three parameters—the molecular weight of a Kuhn step, M_K, the entanglement activity, β, and the Kuhn step frictional time, τ_K—the DSM is able to predict simultaneously both nonlinear rheology and the linear viscoelasticity and dielectric relaxation of monodisperse linear, polydisperse linear and branched polymers[11,21,24,25] and cross-linked networks.[19,49] Recently, a hierarchy of mathematically well-defined slip-link models was developed,[18,50,52] all but one of whose parameters can be obtained from atomistic simulations. Moreover, the most coarse-grained member of the hierarchy, the CFSM, has only two parameters which can be estimated from the low-frequency crossover, (ω_x, G_x), of the dynamic modulus, G^*, of linear monodisperse chains.[51] Here, the CFSM version of the DSM is applied to 1,4-polybutadiene blends of star-branched and linear polymer chains.

In the DSM, polymer chains are described by random walk statistics. This is expected to hold for polymeric chains with contour length and entanglement spacing larger than several Kuhn steps. By assuming that the chain relaxation is slower than the relaxation of a strand between entanglements, the chains are then further coarse-grained to the primitive path defined by the entanglements. The entanglements are randomly distributed along the chain with uniform probability $1/(1 + \beta)$, where $\beta = e^{-\mu^E/k_BT}$, is the "entanglement activity". μ^E is the chemical potential conjugate to the entanglement number, and k_B is the Boltzmann constant. The entanglement activity of the surrounding chains sets the average entanglement density but allows fluctuations in the number of entanglements on the probe chain.

The probe chain is subject to two dynamic processes: sliding dynamics (SD) and constraint dynamics (CD). In SD, Kuhn steps shuffle through slip-links with a characteristic time τ_K. This Kuhn step shuffling between entangled strands is due to Brownian forces and free energy differences. When this process occurs at the ends of a linear chain, or at the free end of a star-branched chain, entanglements can be destroyed or created. The probability of creating an entanglement at the end of the chain is determined by the destruction process through detailed balance. CD is the creation and destruction of entanglements due to SD of the surrounding implicit matrix chains. CD is implemented self-consistently with SD, as described in detail elsewhere.[20] Destruction and creation of entanglements by CD occurs anywhere along the chain. For the star-branched chains, entanglements can be created and destroyed by SD only at the free ends of the star arms and by CD anywhere along the chain.[24] For the linear chains, entanglements are created and destroyed by SD on both ends of the chain and by CD anywhere along the chain.

The characteristic lifetime of the ith entanglement, τ_i^{CD}, is introduced to implement a mean-field self-consistent realization with independent chains in the ensemble. The lifetimes, τ_i^{CD}, are chosen from the distribution of lifetimes, $p^{CD}(\tau_i^{CD})$. This distribution is determined self-consistently from destruction of entanglements by SD. The p^{CD} for the blends considered in this work is given by

$$p^{CD}(\tau^{CD}) = w_{sb}p_{sb}^{CD}(\tau^{CD}) + w_{lc}p_{lc}^{CD}(\tau^{CD}) \quad (1)$$

where w is the weight fraction, and the subindexes sb and lc stand for star-branched and linear chains, respectively. Therefore, in the DSM, each component of the blend is modeled in a self-consistent realization with independent chains in the ensemble. The effect of other chains is given by the self-consistent mean-field defined in eq 1. In other words, in the DSM, each component of the blend, with different architectures, can be realized independently while the effect of other architectures is given by the constraint dynamics mean field.

The DSM is a well-defined mathematical model in which the probability density of chain conformations evolves in time according to a differential Chapman−Kolmogorov equation.[20] To perform calculations of dynamic observables, a probe chain or an ensemble of independent probe chains is evolved in time using a numerical algorithm.[26] The stress tensor is calculated from the simulated chain conformations using an expression derivable from a virtual work argument.[48] Two types of rheological calculations can be performed: equilibrium (or Green−Kubo) calculations in which the rate of deformation tensor is set to zero and the autocorrelation function of stress at equilibrium is followed, or flow calculations in which a specific flow field is applied and the stress as a function of time is recorded.

DOI: 10.1021/acs.macromol.5b02641
Macromolecules 2016, 49, 4964−4977

Using the blend $p^{CD}(\tau^{CD})$, the relaxation modulus for each probe chain in the blend is calculated, and then the blend relaxation modulus, $G(t)$, is expressed in terms of the relaxation modulus of each of the components in the blend as

$$G(t) = w_{sb}G_{sb}(t) + w_{lc}G_{lc}(t) \quad (2)$$

The moduli produced by sliding dynamics without constraint dynamics and that produced by constraint dynamics without sliding dynamics, for the blends studied here, are presented in the Appendix and show that the sliding dynamics, without constraint dynamics, leads to very slow relaxation at long times, as expected. While it is tempting to associate the constraint dynamics function $p^{CD}(\tau^{CD})$ and the corresponding sliding dynamics function of the slip-link model with the time-dependent functions ϕ_{ST} and ϕ of the tube model, no straightforward mapping between the slip-link functions and the time-dependent tube functions has been found to date.

Universality observed in experimental data suggests that the shape of the dynamic modulus of linear, monodisperse, entangled polymers is mostly determined by one parameter, namely the average number of entanglements. This universality has been exploited in predictions of the DSM, which resulted in the development of the clustered fixed slip-link model (CFSM),[25] a less detailed level of description than the DSM, that provides a mapping of β and N_K, the number of Kuhn steps, to one parameter, N_c, the number of clusters. The CFSM is simply the DSM with $\beta = 1$, and by making the following substitutions in the original model

$$M_K \rightarrow M_c \approx 0.56(\beta + 1)M_K \quad (3)$$

$$\tau_K \rightarrow \tau_c \approx 0.265\tau_K\beta^{8/3} \quad (4)$$

where $M_K = M_W/N_K$, $M_c = M_W/N_c$ is the molecular weight of a cluster, τ_c is a cluster-shuffling characteristic time, and M_W is the molecular weight of a chain. Note that τ_c is approximately $\tau_e/4$. The CFSM can describe well both equilibrium viscoelasticity and shear flow for linear and star-branched polymer melts.[25] The CFSM predictions are nearly identical to those of the DSM, and it offers significant computational savings.

IV. RESULTS AND DISCUSSION

IV.1. Tube Model and DSM Predictions for Pure Star and Pure Linear. *IV.1.i. Tube Model Predictions of Dynamic Moduli for Pure Linear and Pure Star Polymers.* Figure 3 shows the WLF shift factors, $a_T(T)$, obtained from shifting the experimental linear viscoelastic G' and G'' curves obtained at various low temperatures to the same reference temperature of 25 °C using TTS for both the star, 24KS and the linear, 58KL samples. The shift factors for the star and linear 1,4-PBd samples are very similar near the reference temperature but differ increasingly with decreasing temperature, especially below −50 °C as seen. This variation in the shift factors at low temperatures can be attributed to a slight difference in the 1,2 content values for the star and linear samples and are well within the limits obtained for 1,4-PBds with 1,2 content ranging between 5 and 11% as recently shown by Park et al.[42] Additionally, the shifted $G'(\omega)$ and $G''(\omega)$ curves for both the 24KS and 58KL samples show good agreement in their high-frequency G' and G'' crossover and superpose very well in the high frequency region as shown in Figure 4, indicating successful time−temperature superposition and that the slight difference in 1,2 content and in low-temperature shift factors does not affect their linear rheology at room temperature. As

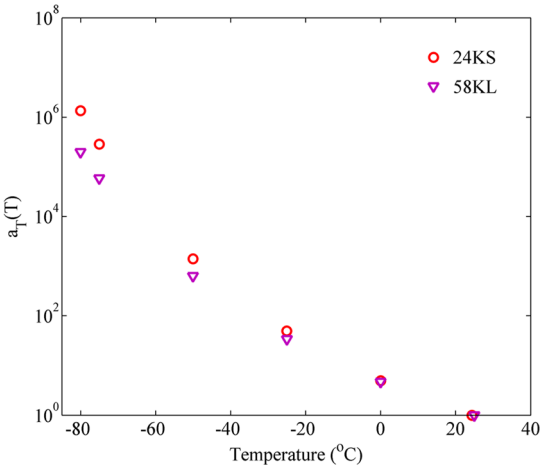

Figure 3. Comparison of the WLF shift factors for 24KS star and 58KL linear 1,4-PBds having the same reference temperature of T = 25 °C.

discussed in Park et al.,[42] the small difference in 1,2 content has negligibly small influence on the plateau modulus and entanglement molecular weight and on the room-temperature entanglement relaxation time τ_e.

Figure 4 features linear viscoelastic G' and G'' relaxation master curves at a reference temperature of 25 °C obtained using TTS for pure monodisperse linear, 58KL and star, 24KS samples. The tube model predictions, from the Hierarchical 3.0 model, which are represented as solid lines in both Figure 4A and Figure 4B, for pure linear and pure star, respectively, are in good agreement with the experimental data, where for the star we assume an arm molar mass of 24 kg/mol rather than the TGIC peak molar mass of 89000/4 = 22.25 kg/mol. The molar mass 24 kg/mol is within experimental error of 22.25 kg/mol, agrees with the SEC molar mass of 97000/4 = 24.25 kg/mol, and gives slightly better agreement with the experimental rheology than does 22.25 kg/mol. Given the demonstrated good success of the tube model in predicting pure star rheology for 1,4-PBd, we believe that the value of 24 kg/mol per arm for the star polymer is accurate. The molar mass of the linear polymer was taken to be the value provided by the supplier, 58 kg/mol. These molar masses were held fixed in all calculations that follow. The good agreement between theory and experiment for pure star and pure linear is not a surprise because various versions of the tube model have done well in predicting monodisperse linear and star polymers.[9]

IV.1.ii. CFSM Model Predictions of Dynamic Moduli for Pure Linear and Pure Star Polymers. Using the procedure described by Katzarova et al.,[51] the two CFSM parameters, τ_c= 0.15 μs and M_c = 618 Da, were obtained by matching the CFSM G^* analytic expressions to the low-frequency crossover (ω_x, G_x) of the linear monodisperse G^* experimental data in Figure 4A. Both of these values are architecture and molecular-weight independent. The DSM parameters for PBd, β = 9.6 and τ_K = 1.3 ns, which are needed to add the Rouse dynamics, were estimated using the scaling relations given in eqs 3 and 4, respectively. A comparison between the prediction using this procedure and experimental data for 58KL at T = 25 °C is shown in Figure 4A as dashed lines. For PBd, M_K = 103.9 Da.[52] The resulting value for the number of clusters is N_c^{lc} = 94. Without further adjustments, these parameters were used for the prediction of the symmetric 4-arm PBd star, 24KS.

DOI: 10.1021/acs.macromol.5b02641
Macromolecules 2016, 49, 4964−4977

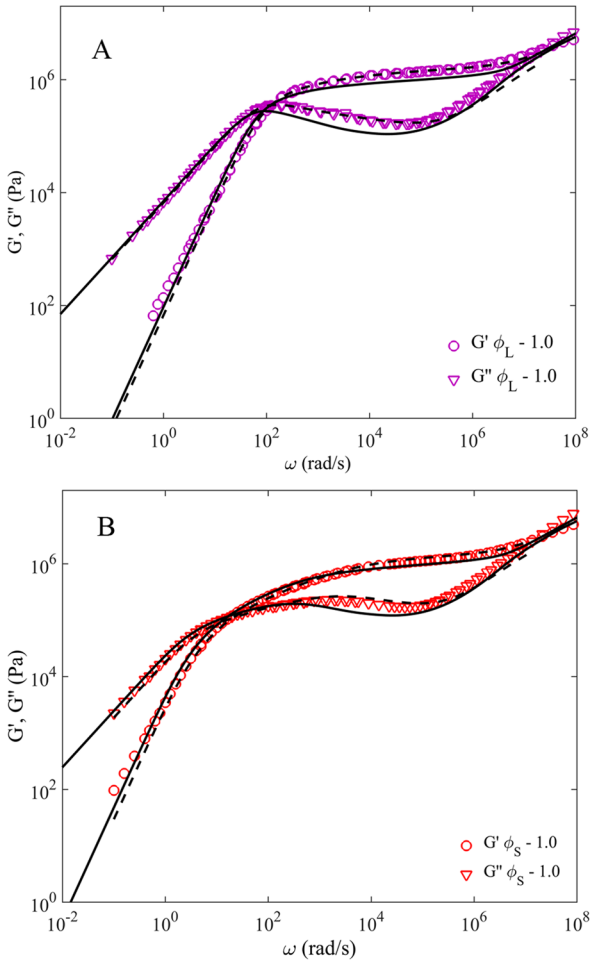

Figure 4. Master curves for storage, G' (circles), and loss, G'' (inverted triangles), moduli for pure 1,4-PBd 58KL linear in (A) and pure 1,4-PBd 24KS star in (B), respectively. The experimental data are time–temperature shifted using the WLF equation and the shift factors from Figure 3 to a reference temperature of T = 25 °C. In both (A) and (B), solid black lines are tube model predictions (Hierarchical 3.0 model) with arm retraction in a "thin" tube in the CR-Rouse regime using the "Park" input parameters given in Table 2. Part A shows CFSM predictions as dashed black lines for pure linear 58KL, which are based on matching the low-frequency crossover data with M_c = 618 Da and τ_e = 0.15 μs. For the star chains, N_c^{sb}/arm = 39, and for the linear chain, N_c^{lc} = 94. Part B shows CFSM predictions (dashed lines) for pure 24K star using the same parameters as in (A).

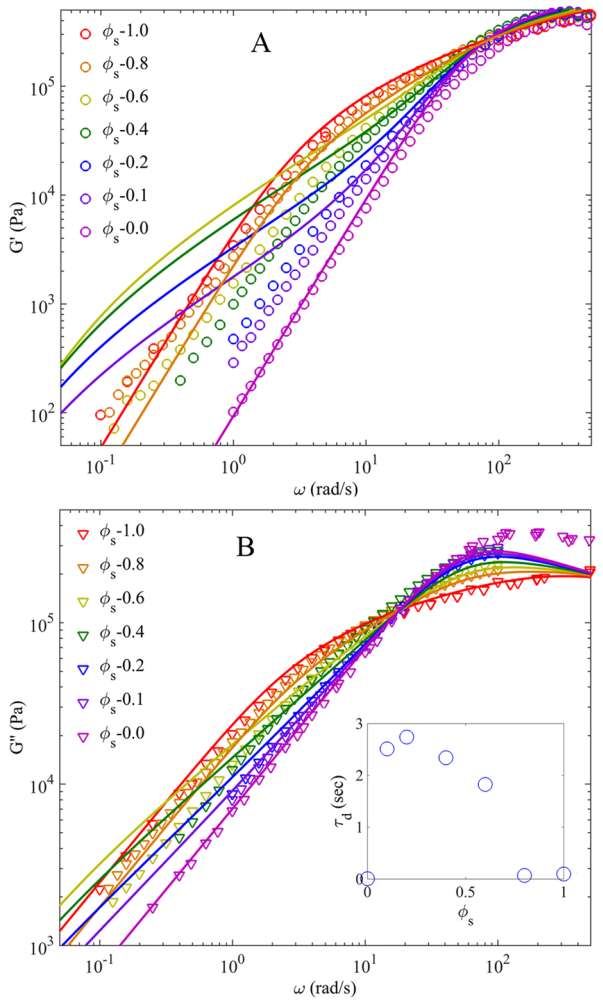

Figure 5. (A) Storage, G' (circles), and (B) loss, G'' (inverted triangles), moduli for PBd 24KS-58KL blends at different star volume fractions as shown. The symbols are experimental data at T = 25 °C. Solid lines are tube model predictions for the same Hierarchical model and parameters described in Figure 4. The inset in (B) shows the variation of terminal time, τ_d, extracted from model predictions as a function of star volume fraction, ϕ_s.

Predictions with β = 1 were done with coarse-grained parameter N_c^{sb}/arm = 39. The resulting prediction is shown in Figure 4B as dashed lines and agrees well in the region of frequencies measured. For both the star and linear chains, the entanglement plateau can be observed at high frequencies. Note that the crossover frequency for the star, which is a rough indicator of the longest relaxation time, occurs at lower frequencies than that for the linear chains since the star chains cannot relax by SD at the branch point.

IV.2. Tube Model and CFSM Slip-Link Predictions for Star/Linear Blends. *IV.2.i. Tube Model Predictions of Dynamic Moduli for Star/Linear Blends.* While the tube model works well for pure 24KS star and for pure 58KL linear polymers with the same model parameters, the model breaks down badly for binary blends of the two, as shown in Figure 5. As can be seen in the G' curves (Figure 5A), for the cases with star fractions ϕ_s = 0.6, 0.4, 0.2, and 0.1, the model predicts a much slower decay in G' in the low-frequency region than is shown in the experimental data. Furthermore, this terminal behavior in G' is slower than even the pure 100% star component. The discrepancy between the experiments and theory is less pronounced in the G'' predictions shown in Figure 5B. The inset in Figure 5B shows the nonmonotonic variation in terminal relaxation time, τ_d, as a function of the star volume fraction, ϕ_s, extracted from Hierarchical model predictions for the same set of data shown in Figure 5. Note that the experimental terminal relaxation times are all less than or equal to that of the pure star and so are more than a decade lower than the predicted values for most of the blends. This massive disagreement between model predictions and experimental data is much larger than shown in the earlier studies of 42.3KS-105KL 1,4-polybutadiene blends,[9] where the tube model at least predicted a monotonic dependence of the terminal relaxation behavior on star volume fraction.

The predictions in Figure 5 are based on the assumption that fluctuations occur in the "thin tube" during CR-Rouse relaxation of the tube. We also tried different versions of the tube model, including fluctuations in the "fat tube", the "arm

DOI: 10.1021/acs.macromol.5b02641
Macromolecules 2016, 49, 4964–4977

frozen" assumption, and the introduction of a "disentanglement" relaxation mechanism to cut off the CR-Rouse process at long times. We also tried the BoB model as well as a "Star–linear" algorithm developed by Park and Larson[57] that implements the original equations of Milner et al.[5] developed for the relaxation of star–linear blends.[5] The results of these attempts are described in the Appendix. Some of the predictions, especially those that invoke disentanglement relaxation, are better than others. The best result is obtained by using disentanglement relaxation when dynamic dilution has reduced the number of entanglements to $S_{a,min} = 2$ (see Figure 6). For 1,4-PBd 24KS-58KL, however, all gave predictions

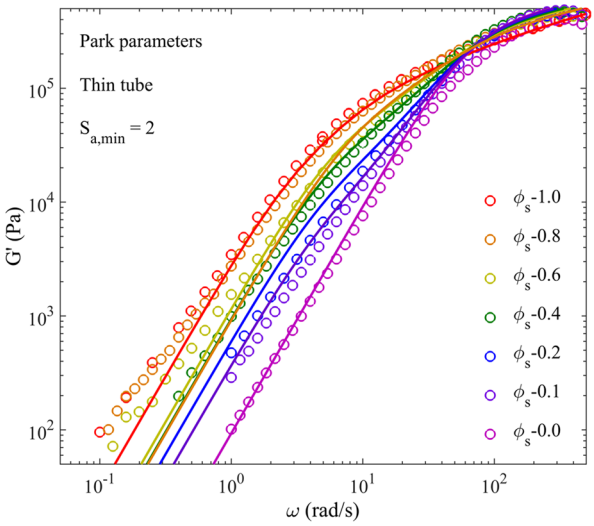

Figure 6. Storage, G', moduli for PBd 24KS-58KL blends at different star volume fractions as shown. The symbols are experimental data at T = 25 °C. Solid lines are Hierarchical tube model predictions with disentanglement relaxation process activated at the entanglement threshold value of $S_{a,min} = 2$.

inferior to the predictions of the slip-link model described next. In addition, in the Appendix, we also test the ability of alternative versions of the tube model, and various alternative input parameter sets, to predict the rheological data for three other sets of star/linear blends available in the literature, namely, that from Struglinski et al.[13] which was also studied by Milner et al.[5] (1,4-PBd 42.3KS-105KL), that of Shivokhin et al.[14] (1,4-PBd 27.4KS-6.9KL), and the data for a single star/linear blend of Roovers[16] (1,4-PBd 342KS-23.6KL). We find that reasonable agreement is obtained with the Hierarchical model with no disentanglement for the two sets of blends in which the pure linear melt relaxes very much faster (by 4 orders of magnitude) than the pure star; this is the case for the blends of Shivokhin et al.[14] (1,4-PBd 27.4KS-6.9KL) and of Roovers[16] (1,4-PBd 342 KS-23.6KL).

This is illustrated in Figure 7, which shows storage moduli predictions for the blends of Shivokhin et al.,[14] 1,4-PBd 27.4KS-6.9KL, using the Hierarchical model, both with and without disentanglement relaxation. For these sets of blends, disentanglement relaxation drastically worsens the agreement with the data as seen in Figure 7. We noted, however, above, in Figure 6, that for 1,4-PBd 24KS-58KL only disentanglement relaxation with an entanglement threshold $S_{a,min} = 2$ is able to bring the tube predictions reasonably close to the data. Thus, the best version of the tube model for 1,4-PBd 24KS-58KL blends produces extremely poor predictions for 1,4-PBd

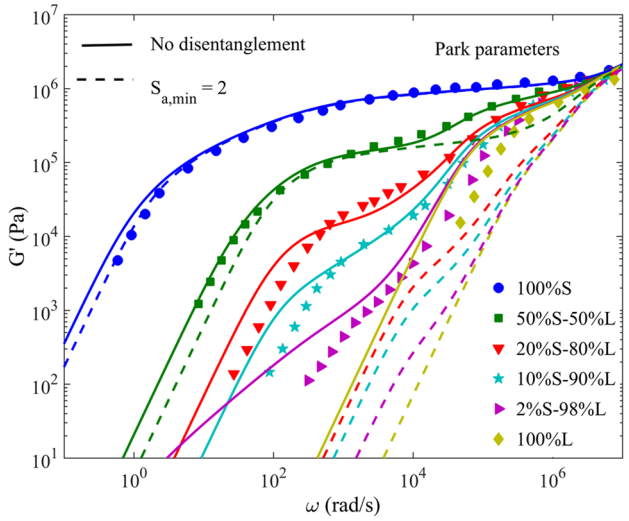

Figure 7. Storage moduli, G', for 1,4-PBd 27.4KS-6.9KL blends at six different star volume fractions as shown. The symbols are experimental data at T = 25 °C. Solid lines show Hierarchical model predictions without the disentanglement process activated, while dashed lines give predictions with disentanglement relaxation process activated at the entanglement threshold value of $S_{a,min} = 2$, both using Park parameters.

27.4KS-6.9KL, and vice versa. Hence, we can conclude that no common current version of the tube model seems able to predict all star/linear blends, even qualitatively. This is confirmed by the extensive comparisons of tube model predictions with star/linear data sets described in the Appendix.

IV.2.ii. CFSM Model Predictions of Dynamic Moduli for Star/Linear Blends. Using the model parameters found in the previous section, for the pure components, the self-consistent CD mean field can be constructed according to eq 1. Then, each type of chain in the ensemble (irrespective of architecture and molecular weight) can be simulated independently using this blend p^{CD} field, eq 1. The relaxation modulus for the blend of star and linear chains is then constructed by performing a weighted average, eq 2, of the relaxation moduli of the two architectures. The parameters, M_c and τ_e, are architecture independent. Therefore, for consistent predictions, the parameters obtained for linear chains were used for the predictions of star/linear blends of 24KS-58KL chains at a reference temperature, T = 25 °C. The dynamic modulus is then obtained by transforming the relaxation modulus to the frequency domain analytically.[51] The resulting storage moduli, G', for each of the different blends as well as 100% star and 100% linear systems are shown in Figure 8A, and the corresponding loss moduli, G'', are shown in Figure 8B.

The CFSM gives considerably improved predictions for bidisperse 24KS-58KL blends over any of the available tube (Hierarchical and BoB) models, as shown in Figure 8. This success may be due to the fact that the CFSM models polymer chain dynamics at a more detailed level than do tube models. Instead of tracking specific constraint release mechanisms and longitudinal motions, the CFSM only tracks the primitive path and fluctuating monomer densities. All CD mechanisms arise naturally, once binary interactions are assumed. As mentioned previously, the model first tracks the movement of Kuhn segments through entanglements without constraint release. The dynamics obtained are then used to construct the constraint release rate, which is used in a second simulation of the sliding dynamics. In this way, the CFSM captures

DOI: 10.1021/acs.macromol.5b02641
Macromolecules 2016, 49, 4964–4977

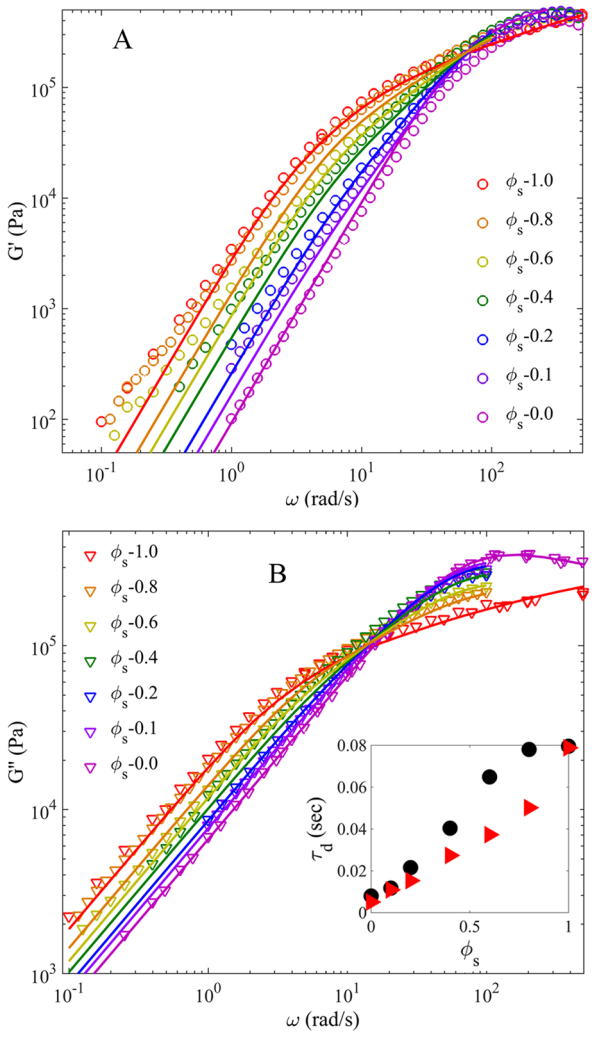

Figure 8. (A) Storage, G' (circles), and loss (B) G'' (inverted triangles), moduli for 1,4-PBd 24KS-58KL blends with decreasing fraction of star-branched chains from *left* to *right* as shown. The symbols are experimental data at T = 25 °C. Solid lines are CFSM predictions. The CFSM parameters used were obtained in section IV.1.ii. For the star-branched chains, N_c^{sb}/arm = 39, and for the linear chain, N_c^{lc} = 94. A self-consistent τ_e = 0.15 μs was used for both architectures. In the inset in (B), red triangles show the variation of terminal time, τ_d, extracted from CFSM predictions, and black circles show terminal time, τ_d, calculated from experimental data as a function of star volume fraction, ϕ_s.

constraint release at a level of detail that eludes the current tube models. We note here that an alternative slip-link model, the "slip-spring" model of Likhtman and co-workers,[14] accounts for constraint release in a single simulation by explicitly pairing a partner matrix chain and one of its slip-links to each slip-link on the "test" chain. Thus, when a new slip-link is created on the test chain when the chain end slides far enough from its last slip-link, a slip-link is also added to a randomly chosen partner chain at a random position. These paired slip-links on both the test chain and the partner chain both disappear only when either the test chain slides through its slip-link or the partner chain slides through its paired slip-link. This "slip-spring" simulation[14] was able to predict successfully the linear rheology of the PBd27.4KS-6.9KL star/linear data set of Shivokhin et al.[14] discussed earlier and can also predict the rheology of our new data set PBd24KS-58KL, as shown in the Appendix, in Figure A18.

We have also applied the CFSM to the PBd27.4KS-6.9KL star/linear blend data of Shivokhin et al.[14] The two CFSM parameters, τ_e = 0.15 μs and M_e = 618 Da, were the same as obtained for the blend 1,4-PBd 24KS-58KL. The reported molar mass of the star arm, 24.5K, in the data set of Shivokhin et al.[14] is only slightly higher than that of the star arm in our work, 24K. Nevertheless, the terminal relaxation of the Shivokhin star is significantly slower than that of our 24K star (see Figure 9). We find that use of a slightly higher molar

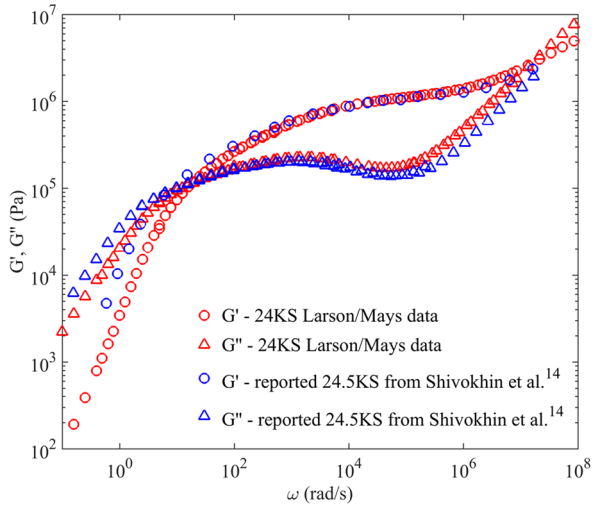

Figure 9. Experimental storage, G' (circles), and loss, G'' (triangles), moduli for pure star 24KS (in red) reported in this work and for pure star 24.5KS (in blue) reported in Shivokhin et al.[14] at 25 °C.

mass, 27.4 kg/mol instead of the reported value of 24.5 kg/mol, gives a slightly better prediction of the pure star relaxation and will therefore be used for the CFSM predictions. We also use a slightly higher value of linear molecular weight, 6.9K, than reported in the paper (6.5K), since the former value was used in the predictions in Shivokhin et al.[14] We have used these slightly higher molecular weights in the Hierarchical predictions, shown in Figure 7, which shifts the results slightly to the left but does not otherwise significantly change the results. (For this reason, these blends are denoted "PBd27.4KS-6.9KL" blends.) Note that this optimized value for the star MW is within uncertainty of the characterization results reported in Shivokhin et al.[14] and agrees with the optimized arm molecular weight used for the slip-spring predictions of the same reference.

Note also in Figure 9 that the high-frequency behavior for the 24.5KS star by Shivokhin et al.[14] is shifted to higher frequency by around a factor of 1.8 and shows a broader frequency range relative to the 24KS star, as seen in the loss modulus curves and are not consistent with one another in the high frequency range. These data are therefore an exception to the universality in previously reported high-frequency 1,4-polybutadiene data in the literature, showing identical behavior at high frequency, regardless of chain length or architecture.[42] This shift in the high-frequency data in the 24.5K star might therefore be due to incomplete temperature equilibration of the sample during rheology measurements at different temperatures. There is also a possibility of differences in the two materials' microstructures, made in two different laboratories,

DOI: 10.1021/acs.macromol.5b02641
Macromolecules 2016, 49, 4964−4977

which might influence the monomer friction coefficient, although such differences would need to be outside the typical range (5−10% 1,2 content) to produce a significant shift.[42]

The molar mass for the linear chains used in the blends of Shivokhin et al.[14] is 6.9 kg/mol. The resulting value for the number of clusters for the linear chains is $N_c^{lc} = 11$. The corresponding parameter used for the prediction of a symmetric 3-arm PBd star-branched melt with optimized arm molar mass M_a = 27.4 kg/mol (PBd27K) is then N_c^{sb}/arm = 44. These parameters were then used for the predictions of blends of PBd27.4K star and PBd6.9K linear chains at a reference temperature of T = 25 °C. The resulting storage, G', moduli for each of the different blends as well as the pure star and linear systems are shown in Figure 10.

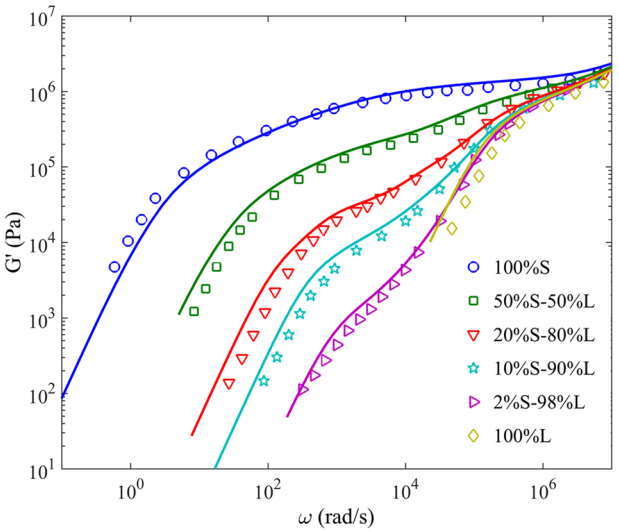

Figure 10. Storage moduli, G', for 1,4-PBd 27.4KS-6.9KL blends (data from Shivokhin et al.[14]) at six different star volume fractions as shown. The symbols are experimental data at T = 25 °C. Solid lines show CFSM predictions. For the star-branched chains, N_c^{sb}/arm = 44, and for the linear chain, N_c^{lc} = 11. A self-consistent τ_c = 0.15 μs was used for both architectures.

Figure 10 shows very successful CFSM prediction for the data set of Shivokhin et al.[14] Both slip-link approaches (the slip-spring simulation of Likhtman and CFSM) can predict both data sets 24KS-58KS and 27.4KS-6.9KS reasonably well (see for example Figure A18 in the Appendix for the prediction of the slip-spring model compared to the data for 24KS-58KS). This suggests that the differences in how these slip-link models handle constraint release do not matter too much at equilibrium and that these slip-link models possess a robustness that is lacking from current tube models. As noted earlier, no version of the model, nor combination of mechanisms and input parameters, was able to predict both our PBd24KS-58KL and the PBd27.4KS-6.9KL sets of blends. In addition, by using the CFSM or slip-spring model to investigate the molecular physics of constraint release in detail, it might be possible to gain an improved understanding that might be captured in a tube model.

V. CONCLUSIONS AND PERSPECTIVE

We have presented a detailed comparison of the linear rheology of carefully synthesized and characterized bidisperse star and linear blends, 24KS-58KL, with both tube-based models (Hierarchical and BoB) and with the recently developed slip-link model, CFSM. While the predictions of the tube models agree in many cases with measured rheological properties for monodisperse linear, star, H, and other polymers, they fail badly for blends of a monodisperse star polymer with a monodisperse linear polymer. Although earlier studies have shown that star/linear blends present problems for tube models, we find here that failure is extreme for our new blends when the star volume fraction is low enough that the star arms are sparsely self-entangled and there are fewer than three entanglements per arm after the relaxation of linear chains.

This failure can be attributed to the inability of the tube models to describe constraint release events accurately in situations where rather abrupt relaxation of a portion of the entanglement network occurs by reptation of linear chains, but the remainder relaxes gradually by arm fluctuations. Tube models with several modifications were used to test the constraint release effects, including (1) using two different sets of input parameters, namely, the Park (α = 4/3) and Das (α = 1) parameters, (2) performing arm retraction in both the *thin* and *fat* tubes in CR-Rouse motion, (3) including a disentanglement mechanism, and (4) using three different computational models, namely, Hierarchical, BoB, and a simple code based on the original set of equations developed by Milner et al.[5] that differ in their numerical implementations but that use the same basic relaxation mechanisms. The only version of the tube model that comes close to predicting the data is one that that invokes "disentanglement relaxation", with the disentanglement threshold adjusted to a best-fit value of $S_{a,min}$ = 2. However, this version performs very poorly for other 1,4-polybutadiene star/linear blend data present in the literature, in particularly the recent data set by Shivokhin et al.[14]

Finally, a slip-link model, the clustered fixed slip-link model (CFSM), proved to be highly successful in predicting the linear rheology of our new set of star−linear blends. It was also successful in describing the rheology of the blends of Shivokhin et al.,[14] which contain a star of similar arm molecular weight to ours but a significantly shorter linear chain. The slip-link model incorporates both sliding dynamics (SD) of individual chains through the entanglement mesh by reptation and contour length fluctuations and constraint dynamics (CD), which captures both the "dynamic dilution" and "constraint-release Rouse" mechanisms of the tube model in simple limiting cases and transcends these mechanisms in more complex situations. The slip-spring model of Likhtman and co-workers worked as well as the CFSM in predicting both data sets, indicating that slip-link models are less sensitive to modeling details and algorithmic implementation as the tube model seems to be for star−linear blends.

Both the CSFM slip-link simulations and the Hierarchical tube models describe relaxation due to sliding dynamics (reptation and contour length fluctuations) of the "test" chain and constraint release due to motion of the matrix chains. In tube models, the sliding dynamics and constraint dynamics are accounted for using a mean-field relaxation function for each of these and then combining these in a rather complex way to produce predictions of stress relaxation. In the CSFM there is a function $p^{CD}(\tau)$ found from "sliding dynamics" which is a probability distribution used for constraint release times. However, there is no attempt to decompose the stress relaxation into a combination of two functions; instead, both constraint release and sliding dynamics are accounted for locally—at each entanglement point in the simulated melt. The

DOI: 10.1021/acs.macromol.5b02641
Macromolecules 2016, 49, 4964−4977

DSM can be used to obtain separate relaxation functions for sliding dynamics and constraint dynamics by turning off respectively the constraint dynamics and the sliding dynamics and computing the resulting relaxation modulus in each case. These modulus functions, each normalized by the zero-time modulus, can be multiplied together to obtain a normalized relaxation modulus, which can be compared to the modulus obtained from the full DSM theory. The idea is to determine if the DSM modulus can be represented as a simple product of moduli produced by sliding dynamics and constraint dynamics. This comparison has been carried out by Khaliullin and Schieber[11] and by Pilyugina et al.[24] and found to work reasonably well for bidisperse linear chains but not for star-branched chains. For the star/linear blends studied here, we carried out analogous tests with the CSFM and find that the factorization fails progressively more severely as the concentration of star polymer increases (results not shown). While the tube models considered here involve computing products of functions describing sliding dynamics and constraint dynamics, even in these tube models the relaxation modulus of a star/linear blend is not a simple product of two such functions because in the tube model constraint dynamics are described using both tube dilation and constraint release Rouse processes, whose relative importance depends on how rapidly constraint release occurs. In fact, the worst failures of the tube model are at the lowest nonzero fraction of star polymer, where factorization, using the DSM model, works best. For pure star or pure linear melts, both CSFM and tube models are successful in predicting linear rheology, and the tube models are not very sensitive to the details of how relaxation is treated during the constraint release Rouse process. For the star/linear blends, however, the sudden release of entanglements that occurs when the linear chains relax while stars are largely unrelaxed exposes the deficiencies of how current tube models manage relaxation that is dominated by constraint release. As discussed in the Appendix, none of the assumptions about relaxation during the period after sudden relaxation of the linear chains give accurate predictions for all available star/linear blends.

Given the much greater computational speed of tube models, however, it would be of great interest to see if there is a deeper understanding of constraint release that can be obtained from a careful interrogation of the CSFM and use this to develop an improved tube model or at least to determine the conditions under which tube models can be expected to be successful and when they cannot be. The possibility of improving the tube model is suggested in some recent studies. For example, recent work by Likhtman and co-workers[54] using a detailed first passage time analysis suggests that the fluctuation time for star arms estimated in Milner et al.[5] and used in most tube models is too slow by a factor of 10 or more. Works by Matsumiya et al.[55] and Matsumiya et al.[56] suggest separating the tube used to compute stress from that used to determine polymer motion, and it may be possible to improve the tube model using such ideas. After all, tube models such as the Hierarchical model and the BoB model have successfully predicted the rheology of many polymer melts, including compositionally complex commercial melts.[6,53] Commercial polymers are invariably polydisperse, and it appears that the severe errors that occur when applying tube models to blends of monodisperse stars with monodisperse linear polymer are not nearly as severe for polymers with broad polydispersity. However, without either an improvement in the underlying description of constraint release in tube models or at least a clear delineation of the conditions under which tube models will and will not work well, we must remain skeptical of their reliability.

■ ASSOCIATED CONTENT

Supporting Information

The Supporting Information is available free of charge on the ACS Publications website at DOI: 10.1021/acs.macromol.5b02641.

Appendix (PDF)

■ AUTHOR INFORMATION

Corresponding Author

*E-mail rlarson@umich.edu (R.G.L.).

Author Contributions

P.S.D., B.-G.K., and M.K. contributed equally to this work.

Notes

The authors declare no competing financial interest.

■ ACKNOWLEDGMENTS

P.S.D. and R.G.L. gratefully acknowledge the support of the National Science Foundation under Grant DMR 1403335. Any opinions, findings, and conclusions or recommendations expressed in this material are those of the authors and do not necessarily reflect the views of the National Science Foundation (NSF). J.M. and B.-G.K. acknowledge partial support by the U.S. Department of Energy, Office of Science, Basic Energy Sciences, Materials Sciences and Engineering Division. T.C. acknowledges the support from the National Research Foundation of Korea (NRF) (2012R1A2A2A01015148 and 2015R1A2A2A01004974). J.D.S. acknowledges support from the Army Research office (W911NF-11-2-0018) and the National Science Foundation (NSF CBET 1336442).

■ REFERENCES

(1) de Gennes, P. G. Reptation of a Polymer Chain in the Presence of Fixed Obstacles. *J. Chem. Phys.* **1971**, *55*, 572.

(2) Doi, M.; Edwards, S. F. *The Theory of Polymer Dynamics*, 2nd ed.; Clarendon: Oxford, 1988.

(3) Viovy, J. L.; Rubinstein, M.; Colby, R. H. Constraint Release in Polymer Melts: Tube Reorganization Versus Tube Dilation. *Macromolecules* **1991**, *24*, 3587.

(4) Marrucci, G. Relaxation by Reptation and Tube Enlargement: A Model for Polydisperse Polymers. *J. Polym. Sci., Polym. Phys. Ed.* **1985**, *23*, 159.

(5) Milner, S. T.; McLeish, T. C. B.; Young, R. N.; Hakiki, A.; Johnson, J. M. Dynamic Dilution, Constraint-Release, and Star-Linear Blends. *Macromolecules* **1998**, *31*, 9345.

(6) Das, C.; Inkson, N. J.; Read, D. J.; Kelmanson, M. A.; McLeish, T. C. B. Computational Linear Rheology of General Branch-On-Branch Polymers. *J. Rheol.* **2006**, *50*, 207.

(7) Larson, R. G. Combinatorial Rheology of Branched Polymer Melts. *Macromolecules* **2001**, *34*, 4556.

(8) Park, S. J.; Shanbhag, S.; Larson, R. G. A Hierarchical Algorithm for Predicting the Linear Viscoelasticity of Polymer Melts with Long-Chain Branching. *Rheol. Acta* **2005**, *44*, 319.

(9) Wang, Z.; Chen, X.; Larson, R. G. Comparing Tube Models for Predicting the Linear Rheology of Branched Polymer Melts. *J. Rheol.* **2010**, *54*, 223.

(10) van Ruymbeke, E.; Masubuchi, Y.; Watanabe, H. Effective Value of the Dynamic Dilution Exponent in Bidisperse Linear Polymers: From 1 to 4/3. *Macromolecules* **2012**, *45* (4), 2085.

(11) Khaliullin, R. N.; Schieber, J. D. Application of the Slip-Link Model to Bidisperse Systems. *Macromolecules* **2010**, *43*, 6202.

DOI: 10.1021/acs.macromol.5b02641
Macromolecules 2016, 49, 4964−4977

(12) Watanabe, H. Slow Dynamics in Homopolymer Liquids. *Polym. J.* **2009**, *41*, 929.
(13) Struglinski, M. J.; Graessley, W. W.; Fetters, L. J. Effects of Polydispersity on the Linear Viscoelastic Properties of Entangled Polymers. 3. Experimental Observations on Binary Mixtures of Linear and Star Polybutadienes. *Macromolecules* **1988**, *21*, 783.
(14) Shivokhin, M. E.; van Ruymbeke, E.; Bailly, C.; Kouloumasis, D.; Hadjichristidis, N.; Likhtman, A. E. Understanding Constraint Release in Star/Linear Polymer Blends. *Macromolecules* **2014**, *47*, 2451.
(15) Lee, J. H.; Archer, L. A. Stress Relaxation of Star/Linear Polymer Blends. *Macromolecules* **2002**, *35*, 6687.
(16) Roovers, J. Tube Renewal in the Relaxation of 4-arm-star Polybutadienes in Linear Polybutadienes. *Macromolecules* **1987**, *20*, 148.
(17) Masubuchi, Y. Simulating the Flow of Entangled Polymers. *Annu. Rev. Chem. Biomol. Eng.* **2014**, *5*, 11.
(18) Schieber, J. D.; Andreev, M. Entangled Polymer Dynamics in Equilibrium and Flow Modeled through Slip Links. *Annu. Rev. Chem. Biomol. Eng.* **2014**, *5*, 367.
(19) Jensen, M. K.; Khaliullin, R.; Schieber, J. D. Self-Consistent Modeling of Entangled Network Strands and Linear Dangling Structures in a Single-Strand Mean-Field Slip-Link Model. *Rheol. Acta* **2012**, *51*, 21.
(20) Khaliullin, R. N.; Schieber, J. D. Self-Consistent Modeling of Constraint Release in a Single-Chain Mean-Field Slip-Link Model. *Macromolecules* **2009**, *42*, 7504.
(21) Andreev, M.; Khaliullin, R. N.; Steenbakkers, R. J.; Schieber, J. D. Approximations of the Discrete Slip-Link Model and their Effect on Nonlinear Rheology Predictions. *J. Rheol.* **2013**, *57*, 535.
(22) Schieber, J. D. Fluctuations in Entanglements of Polymer Liquids. *J. Chem. Phys.* **2003**, *118*, 5162.
(23) Likhtman, A. E. Single-Chain Slip-Link Model of Entangled Polymers: Simultaneous Description of Neutron Spin−Echo, Rheology, and Diffusion. *Macromolecules* **2005**, *38* (14), 6128.
(24) Pilyugina, E.; Andreev, M.; Schieber, J. D. Dielectric Relaxation as an Independent Examination of Relaxation Mechanisms in Entangled Polymers Using the Discrete Slip-Link Model. *Macromolecules* **2012**, *45*, 5728.
(25) Andreev, M.; Feng, H.; Yang, L.; Schieber, J. D. Universality and Speedup in Equilibrium and Nonlinear Rheology Predictions of the Fixed Slip-Link Model. *J. Rheol.* **2014**, *58*, 723.
(26) Andreev, M.; Schieber, J. D. Accessible and Quantitative Entangled Polymer Rheology Predictions, Suitable for Complex Flow Calculations. *Macromolecules* **2015**, *48* (5), 1606.
(27) Pattamaprom, C.; Larson, R. G. Predicting the Linear Viscoelastic Properties of Monodisperse and Polydisperse Polystyrenes and Polyethylenes. *Rheol. Acta* **2001**, *40*, 516.
(28) Hadjichristidis, N.; Iatrou, H.; Pispas, S.; Pitsikalis, M. Anionic Polymerization: High Vacuum Techniques. *J. Polym. Sci., Part A: Polym. Chem.* **2000**, *38*, 3211.
(29) Uhrig, D.; Mays, J. W. Experimental Techniques in High-Vacuum Anionic Polymerization. *J. Polym. Sci., Part A: Polym. Chem.* **2005**, *43*, 6179.
(30) Rahman, M. S.; Aggarwal, R.; Larson, R. G.; Dealy, J. M.; Mays, J. Synthesis and Dilute Solution Properties of Well-Defined H-Shaped Polybutadienes. *Macromolecules* **2008**, *41*, 8225.
(31) Rahman, M. S.; Lee, H.; Chen, X.; Chang, T.; Larson, R.; Mays, J. Model Branched Polymers: Synthesis and Characterization of Asymmetric H-Shaped Polybutadienes. *ACS Macro Lett.* **2012**, *1*, 537.
(32) Chang, T. Polymer Characterization by Interaction Chromatography. *J. Polym. Sci., Part B: Polym. Phys.* **2005**, *43*, 1591.
(33) Ryu, J.; Chang, T. Thermodynamic Prediction of Polymer Retention in Temperature-Programmed HPLC. *Anal. Chem.* **2005**, *77*, 6347.
(34) Lee, W.; Park, S.; Chang, T. Liquid Chromatography at the Critical Condition for Polyisoprene Using a Single Solvent. *Anal. Chem.* **2001**, *73*, 3884.
(35) Lee, H. C.; Lee, W.; Chang, T.; Yoon, J. S.; Frater, D. J.; Mays, J. W. Linking Reaction Kinetics of Star Shaped Polystyrene by Temperature Gradient Interaction Chromatography. *Macromolecules* **1998**, *31*, 4114.
(36) Perny, S.; Allgaier, J.; Cho, D.; Lee, W.; Chang, T. Synthesis and Structural Analysis of an H-Shaped Polybutadiene. *Macromolecules* **2001**, *34*, 5408.
(37) Ratkanthwar, K.; Hadjichristidis, N.; Lee, S.; Chang, T.; Pudukulathan, Z.; Vlassopoulos, D. Synthesis and Characterization of an Exact Comb Polyisoprene with Three Branches Having the Middle Branch Twice the Molecular Weight of the Other Two Identical External Branches. *Polym. Chem.* **2013**, *4*, 5645.
(38) Lee, H. C.; Chang, T.; Harville, S.; Mays, J. W. Characterization of Linear and Star Polystyrene by Temperature-Gradient Interaction Chromatography with a Light-Scattering Detector. *Macromolecules* **1998**, *31*, 690.
(39) Chen, X.; Rahman, S.; Lee, H.; Mays, J.; Chang, T.; Larson, R. Combined Synthesis, TGIC Characterization, and Rheological Measurement and Prediction of Symmetric H Polybutadienes and Their Blends with Linear and Star-Shaped Polybutadienes. *Macromolecules* **2011**, *44*, 7799.
(40) Im, K.; Park, S.; Cho, D.; Chang, T.; Lee, K.; Choi, N. HPLC and MALDI-TOF MS Analysis of Highly Branched Polystyrene: Resolution Enhancement by Branching. *Anal. Chem.* **2004**, *76*, 2638.
(41) Kim, Y.; Ahn, S.; Chang, T. Martin's Rule for High-Performance Liquid Chromatography Retention of Polystyrene Oligomers. *Anal. Chem.* **2009**, *81*, 5902.
(42) Park, S. J.; Desai, P. S.; Chen, X.; Larson, R. G. Universal Relaxation Behavior of Entangled 1,4-polybutadiene Melts in the Transition Frequency Region. *Macromolecules* **2015**, *48*, 4122.
(43) Colby, R. H.; Rubinstein, M. Two-Parameter Scaling for Polymers in Solvents. *Macromolecules* **1990**, *23*, 2753.
(44) Milner, S. T.; McLeish, T. C. B. Parameter-Free Theory for Stress Relaxation in Star Polymer Melts. *Macromolecules* **1997**, *30*, 2159.
(45) Milner, S. T. Predicting the Tube Diameter in Melts and Solutions. *Macromolecules* **2005**, *38*, 4929.
(46) Neergaard, J.; Schieber, J. D. A Full-Chain Network Model with Sliplinks and Binary Constraint Release*Proc. XIIIth Int. Cong. Rheol.*, 2000.
(47) Schieber, J. D.; Neergaard, J.; Gupta, S. A Full-Chain, Temporary Network Model with Sliplinks, Chain-Length Fluctuations, Chain Connectivity and Chain Stretching. *J. Rheol.* **2003**, *47*, 213.
(48) Schieber, J. D. GENERIC Compliance of a Temporary Network Model with Sliplinks, Chain-Length Fluctuations, Segment-Connectivity and Constraint Release. *J. Non-Equilib. Thermodyn.* **2003**, *28*, 179.
(49) Katzarova, M.; Andreev, M.; Sliozberg, Y. R.; Mrozek, R. A.; Lenhart, J. L.; Andzelm, J. W.; Schieber, J. D. Rheological predictions of network systems swollen with entangled solvent. *AIChE J.* **2014**, *60*, 1372.
(50) Schieber, J. D.; Indei, T.; Steenbakkers, R. J. A. Fluctuating Entanglements in Single-Chain Mean-Field Models. *Polymers* **2013**, *5*, 643.
(51) Katzarova, M.; Yang, L.; Andreev, M.; Córdoba, A.; Schieber, J. D. Analytic Slip-Link Expressions for Universal Dynamic Modulus Predictions of Linear Monodisperse Polymer Melts. *Rheol. Acta* **2015**, *54*, 169.
(52) Steenbakkers, R. J.; Tzoumanekas, C.; Li, Y.; Liu, W. K.; Kröger, M.; Schieber, J. D. Primitive-Path Statistics of Entangled Polymers: Mapping Multi-Chain Simulations onto Single Chain Mean-Field Models. *New J. Phys.* **2014**, *16*, 015027.
(53) Chen, X.; Costeux, C.; Larson, R. G. Characterization and Prediction of Long-Chain Branching in Commercial Polyethylenes by a Combination of Rheology and Modeling Methods. *J. Rheol.* **2010**, *54* (6), 1185.
(54) Cao, J.; Zhu, J.; Wang, Z.; Likhtman, A. E. Large Deviations of Rouse Polymer Chain: First Passage Problem. *J. Chem. Phys.* **2015**, *143*, 204105.

DOI: 10.1021/acs.macromol.5b02641
Macromolecules 2016, 49, 4964−4977

(55) Matsumiya, Y.; Kumazawa, K.; Nagao, M.; Urakawa, O.; Watanabe, H. Dielectric Relaxation of Monodisperse Linear Polyisoprene: Contribution of Constraint Release. *Macromolecules* **2013**, *46*, 6067.
(56) Matsumiya, Y.; Masubuchi, Y.; Inoue, T.; Urakawa, O.; Liu, C. Y.; van Ruymbeke, E.; Watanabe, H. Dielectric and Viscoelastic Behavior of Star-Branched Polyisoprene: Two Coarse-Grained Length Scales in Dynamic Tube Dilation. *Macromolecules* **2014**, *47*, 7637.
(57) Park, S. J.; Larson, R. G. Dilution Exponent in the Dynamic Dilution Theory for Polymer Melts. *J. Rheol.* **2003**, *47*, 199.
(58) Ramirez, J.; Sukumaran, S. K.; Likhtman, A. E. Significance of Cross Correlations in the Stress Relaxation of Polymer Melts. *J. Chem. Phys.* **2007**, *126* (24), 244904.
(59) Likhtman, A. E. *Viscoelasticity and Molecular Rheology*; Elsevier B.V.: Amsterdam, 2012; p 133.
(60) Qiao, X. Y.; Sawada, T.; Matsumiya, Y.; Watanabe, H. Constraint Release in Moderately Entangled Monodisperse Star Isoprene Systems. *Macromolecules* **2006**, *39*, 7333.

DOI: 10.1021/acs.macromol.5b02641
Macromolecules 2016, 49, 4964−4977